Jurnal Kejuruteraan 37(5) 2025: 2521-2536
https://doi.org/10.17576/jkukm-2025-37(5)-37

Design and Modeling of the Gyro Plate for Marine Gyrostabilizer Using Finite Element Analysis

Harith Aslam Ahmad Naziri[a], Ahmad Imran Ibrahim[a*] & Zulkifli Zainal Abidin[a]

[a]*Department of Mechatronics Engineering, International Islamic University Malaysia (IIUM)*

[*]*Corresponding author: imran@iium.edu.my*

Received 11 July 2024, Received in revised form 22 April 2025
Accepted 22 May 2025, Available online 30 August 2025

ABSTRACT

Marine vessels experience motion in six degrees of freedom, particularly during adverse weather conditions such as storms, heavy rain, rough seas, and strong winds. Gyroscopic stabilizers offer a promising solution to mitigate these motions, as they are unaffected by hydrodynamic drag and external factors like seaweed. This study focuses on the development and optimization of the gyro plate, a critical component of the gyrostabilizer system. Five gyro plate models, inspired by a published design from prior research, were created and analyzed using Finite Element Analysis (FEA) in SOLIDWORKS. The methodology included a mesh curvature study to ensure the accuracy of stress, deformation, and strain predictions under static loads. The results demonstrated progressive improvements from Models 1 to 5, with Model 5 emerging as the optimal design. For PLA Pro material, Model 5 achieved the lowest stress (2.18 MPa), minimal deformation (0.618 mm), and reduced strain, enhancing structural efficiency by minimizing stress concentrations and evenly distributing loads. While Models 1 and 2 stood out for their simplicity and cost-effective manufacturability, Model 5 balanced superior performance with high compatibility for 3D printing, requiring minimal post-processing. This study highlights the structural efficiency, reduced displacement, and manufacturability of the optimized gyro plate, paving the way for improved gyroscopic stabilization systems. The findings contribute to more efficient and reliable marine transportation, with potential applications for larger vessels.

Keywords: Gyro plate; optimal design; Finite Element Analysis (FEA)

INTRODUCTION

The Gyro Plate, also known as a gimbal, is a crucial component in marine gyrostabilizers. Gyro plates play a significant role in stabilizing marine vessels by providing optimal design and modeling using finite element analysis. This technology involves a multi-degree gimbal system that enhances stability and precision in marine applications (Md Tahir et al. 2011). The gyro plate's design is essential for controlling vibrations and disturbances in marine environments, ensuring the smooth operation of the gyrostabilizer system (Nguyen et al. 2022). Additionally, gyro plate is a part that the precessional motion acted on it in most of the time upon wave and other disturbances excited on it, causing the marine vehicle to roll (Arutyunov, 1960;Jianhui & Shaonan 2011).

Finite element analysis (FEA) is a key method used in the design and modeling of gyro plates, allowing for accurate simulations and validations of the structural integrity and performance of these components (Md Tahir et al. 2011). This approach ensures that the gyro plate can withstand the dynamic forces experienced in marine environments, contributing to the overall efficiency and reliability of the gyrostabilizer system. Understanding and optimizing the design of the gyro plate are essential to enhance the stability and performance of marine vessels upon its anti-rolling operation. It is important to note that the optimal design in Finite Element Analysis aims to minimize stress, deformation, and strain within a structure, leading to improved performance and reliability (Pavlidis & Rowe n.d.).

In this paper, five models of gyro plate to fit 1-meter vessel were designed in SOLIDWORKS, adapted from a previously published design to refine and improve

performance. The dimension of the gyro plate design in this study modelled to fit 1-meter vessel. Finite Element Analysis (FEA) was performed on each model under specified static loading conditions to evaluate equivalent stress, total deformation, and principal strain. The objective of this study is to identify the most optimal design among the models by comparing their performance metrics and selecting the design that achieves the best balance of stress reduction, minimal displacement, and strain under the given conditions.

REQUIREMENT OF GYROSTABILIZER

The hardware requirements for a gyrostabilizer system typically include components such as a high-speed rotating flywheel, gyroscopic sensors, control systems, and actuators. Regardless of ground, marine, or space purposes, gyrostabilizer shares a fundamental mechanical construction comprising of flywheel driven by an actuator (usually a high-speed motor), a gimbal plate, and a damper or actuator (Naziri & Ibrahim 2022) as shown in Figure 1 below.

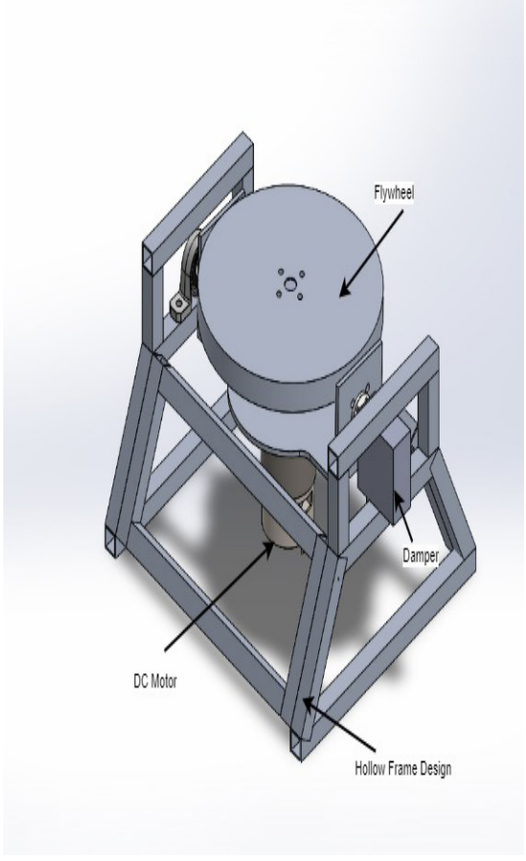

FIGURE 1. Gyrostabilizer (Naziri & Ibrahim 2022)

Furthermore, gyrostabilizers may also feature gyroscopic sensors to detect angular deviations and provide feedback for the control system to adjust the stabilizing forces (Yudachev et al. 2021). Actuators are essential for translating the control signals into mechanical actions to counteract rolling motion effectively (Wang et al. 2017). These hardware components work in synergy to ensure that the gyrostabilizer system can effectively stabilize the marine vessel by generating opposing moments to counter external forces, such as wave-induced disturbances (Deleanu et al. 2022).

REACTION OF SCIENCE OF GYROSTABILIZER.

The gyrostabilizer, also known as the anti-rolling gyrostabilizer device, operates based on the principle of angular momentum conservation. The gyro disc or flywheel in the middle is a vital component of a marine gyrostabilizer system, essential for stabilizing the vessel through the application of gyroscopic principles. The gyro plate rotates rapidly, generating angular momentum that counteracts the ship's rolling motion, thereby improving stability (Li et al. 2022). In the modern design of gyrostabilizer, a control method is implemented on the precessional motion of the gyrostabilizer to effectively counteract the rolling motion, thus helping the vessel to maintain an upright position (Beznos et al. 1998).

FINITE ELEMENT ANALYSIS OF GYRO PLATE

Finite Element Analysis (FEA) has evolved significantly since its inception by Richard Courant in the early 1940s (Liu et al. 2022), transitioning from a method primarily focused on traditional engineering materials, such as metals, to a versatile analytical tool applicable to a broad spectrum of materials, including composites, polymers, and ceramic (Virág & Szirbik 2021). This evolution has been fueled by advancements in computational technology, which have enabled engineers and researchers to simulate complex physical phenomena across various domains, including solid and fluid mechanics, structural analysis, and dynamic response assessments (Hung et al. 2021). In the context of marine gyrostabilizers, FEA plays a pivotal role in the design and optimization of the Gyro Plate, which is critical for ensuring the stability and performance of marine vessels in turbulent conditions.

Finite element analysis serves as a fundamental tool in the design and modelling process of the Gyro Plate,

allowing for accurate simulations and assessments of its response to various loads and conditions. By incorporating von Mises stress, deformation, and strain analyses into the finite element models, engineers can optimize the design of the Gyro Plate to ensure it can withstand the dynamic forces encountered in marine environments (Müller et al. 2008; Nurrohmad et al. 2024). Moreover, the Gyro Plate's ability to mitigate stresses, deformations, and strains is critical for maintaining the operational efficiency and longevity of marine gyrostabilizers. By focusing on these key factors during the design and modelling phase, engineers can enhance the performance and durability of the Gyro Plate, thereby improving the overall stability and functionality of the gyrostabilizer system in challenging marine conditions (Lenartowicz et al. 2021).

In practical applications, FEA is often conducted using software such as SOLIDWORKS, which integrates CAD capabilities with robust FEA tools. This software facilitates a direct method of discretizing the Gyro Plate into finite elements (Jagota et al. 2013) , allowing for the resolution of complex equations that govern its behavior under various loading scenarios (S. Zhang et al. 2024). SOLIDWORKS provides a user-friendly interface for mesh generation and analysis, enabling engineers to conduct iterative design refinements efficiently. The reliability of the results obtained from FEA in SOLIDWORKS is attributed to its ability to handle intricate geometries and boundary conditions, yielding critical insights into stress distribution, displacement, and strain behavior (Diniz et al. 2021). Such insights are invaluable for validating and optimizing the engineering designs of the Gyro Plate, ensuring that it meets the rigorous demands of marine applications.

METHODOLOGY

The importance of optimal design of gyro plate to be simulated is to find the best and optimal design in terms of its less bending or deformation. First, the three-dimensional Computer-Aided-Design (CAD) models of the different gyro plate design were modeled in SOLIDWORKS, and it is simulated using SOLIDWORKS Simulation tool of static analysis. Next step, the materials for the whole gyro plate are selected, the fixtures are set, and the external loads comprises of gravitational acceleration, motor loads of 3.47N and flywheel of 9.64N in the middle of gyro plate. The results of the computational analysis such as equivalent von misses stress, total deformation, maximum principal strain, were computed. If the results have the most improvement in those aspects and cost to make it feasible and acceptable, then the model and its material type is selected and preferred. The flow chart of the approach used to carry out the project is illustrated in Figure 2.

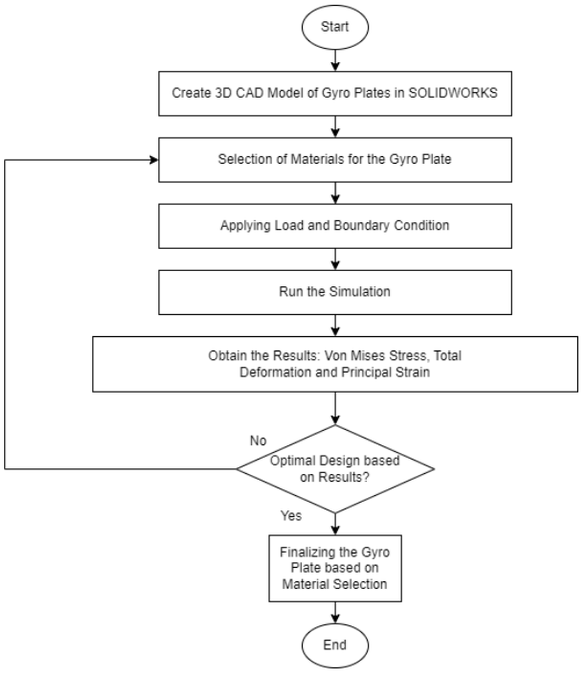

FIGURE 2. Methodology of Flowchart.

MODELLING OF GYRO PLATE

The five distinct gyro plate models, each with differing design, were created in SOLIDWORKS utilizing the sketch tool and the Extruded Base/Boss feature within the SOLIDWORKS Part environment. The form and representation adhere to the established standard gyro plate design of a gyrostabilizer, tailored specifically for stabilization applications are adapted from self-stabilization of ground vehicle. For example Gogoi et al. (2017) and Park & Cho (2018) presents a self-balancing gyrostabilizer on a two-wheel vehicle and a robot respectively while Karagiannis (2015) and T. A. O. Zhang (2014), uniquely developed gyrostabilizer on an amphibious vehicle themselves. Other than ground stabilization, there are also marine vessel gyro-stabilization such as on ship (Talha et al. 2017), barge (Manmathakrishnan & Pannerselvam 2019), as well as self-stabilization for vehicle in space (Lee, 2015) in previous research. Subsequently, the entire assembly was constructed using SOLIDWORKS Assembly. Detailed CAD models and drawings for individual components and the assembled gyro plate model are provided in this section.

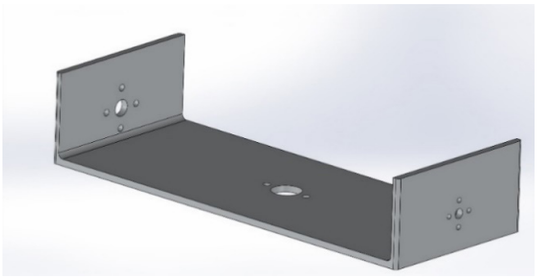

FIGURE 3. Model 1

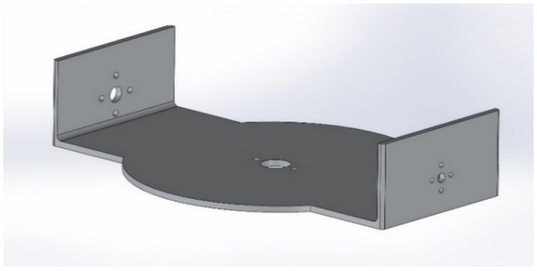

FIGURE 4. Model 2

Figures 3, 4, 5, 6 and 7 depict the five diverse gyro plate models. Model 1 as in Figure 3 is the simplest model among all, where merely holes for two actuators (high speed motor and precession motor) and a bearing mounting are designed and adopted from most of the early research related to gyro plate (Gogoi et al. 2017). Next, model 2 shown in Figure 4 has a curved shape on the flat side where the high-speed motor is mounted. In model 3 as presented in Figure 5, the gyro plate has two support plates on the right and left side towards the bottom, resembling a simulation-based research of simplified marine hull model (Poh et al. 2018). On the other hand, model 4 is designed to mimic field test research of barge (Manmathakrishnan & Pannerselvam, 2019) where the flywheel or gyro itself is surrounded fully with extra top cover added. Lastly, the gyro plate design of model 5 is designed in a way that the triangular support structure gusset-like shape at the corner left and right of gyro plate as shown in Figure 7.

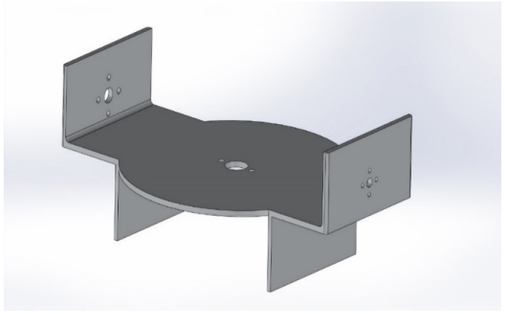

FIGURE 5. Model 3

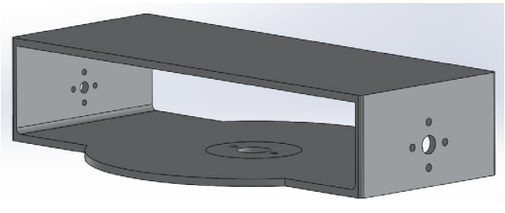

FIGURE 6. Model 4

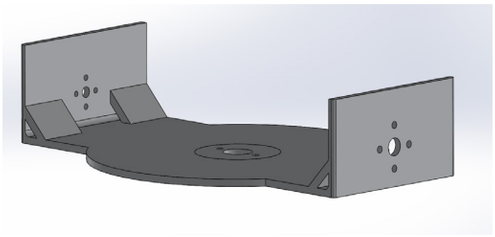

FIGURE 7. Model 5

Figures 8 and 9 show the assembled model of gyro plate with actuators mounted on it and full installation of the gyrostabilizer on a 1-meter vessel, respectively. As portrayed in the figure, two actuators are necessary in gyrostabilizer design, each for generating momentum and controlling precessional motion to counteract the excited external forces.

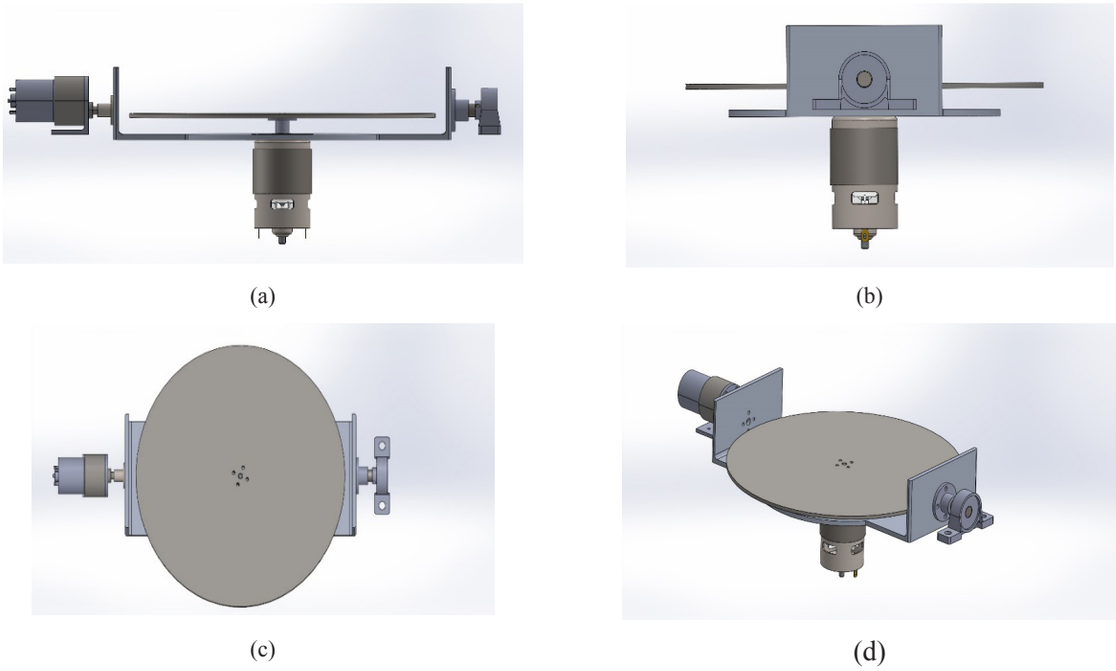

FIGURE 8. Assembly of Gyro Plate with the Actuators. (a) Front View (b) Right View (c) Top View (d) Isometric View

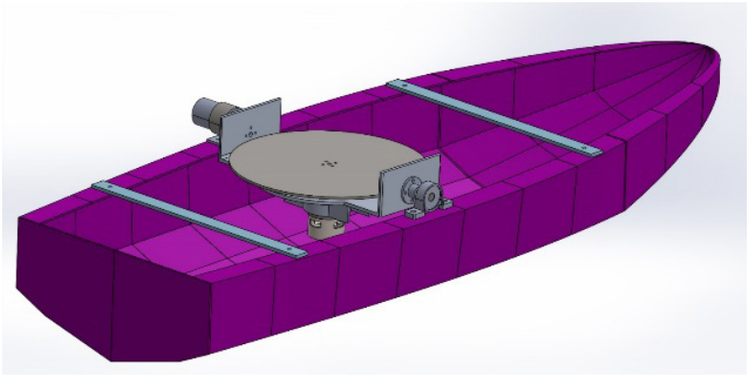

FIGURE 9. Installation of The Gyrostabilizer on the Vessel

ANALYSIS

FINITE ELEMENT ANALYSIS

FEA is conducted on SOLIDWORKS, after modelling the gyro plate using static analysis in simulation to obtain the results of von Mises Stress and total deformation.

MATERIAL SELECTION

The various materials such as Polylactic Acid (PLA) plastic, 1060 Aluminium Alloy and ASTM 36 or mild steel are selected for gyro plate's part and analyses are performed. The selection of the materials and their properties for each part are shown in Table 1.

TABLE 1. Material Properties of Simulated Gyro Plate

Materials Used	Density (Kg/m^3)	Tensile yield strength (MPa)	Tensile ultimate strength (MPa)	Young modulus (MPa)	Poison ratio
PLA	1020	26.082	32.938	2000	0.394
1060 Aluminium Alloy	2700	27.5742	68.9356	6.9 x 104	0.33
Mild Steel	7860	250	400	206 x 103	0.3

LOADING AND BOUNDARY CONDITION

In SOLIDWORKS Simulation, loading conditions refer to the applied forces, pressures, temperatures, etc., that act on the model. In this research case, gravitational acceleration, force due to the hanging high-speed motor and flywheel weight are set to -9.81m/s^2, 3.47247N and 9.647154N respectively. These values and representation of loading and boundary condition are shown in Table 2 and Figure 10 below. The motor and bearing mounted on the two-end of the gyro plate presented have no significant value in term of load in this simulation as they are fixed, hence not available (N/A) status is mentioned in the table.

TABLE 2. Loading and Boundary Condition Components

SI. No	Components	Value
1	Gravitational Acceleration (Red)	-9.81 m/s2
2	Motor (Purple)	3.47247N
3	Flywheel/Disc (Turqoise)	9.647154N
4	Fixed Motor and Bearing Mounting (Green Color)	N/A

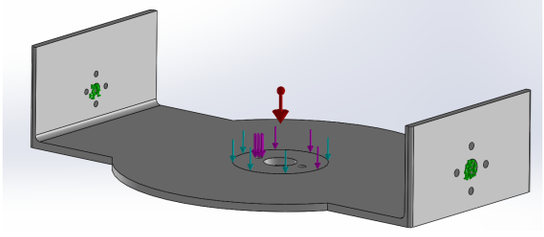

FIGURE 10. Loading and Boundary Conditions.

MESH CONVERGENCE

After conducting preliminary analysis on mesh comparison study with different meshing settings available on SOLIDWORKS it was determined that choosing curvature-based mesh is the optimal type for FEA due to the presence of fillets and holes in the design. Additionally, the design of the model is not overly complex, making the use of blended curvature-based mesh unnecessary. In this study, an example of PLA PRO is selected for material and a critical point of stress is observed and selected at the entities on the edge of the high-speed motor mount in the middle hole at the bottom of the gyro plate. This is to provide consistency during the observation of the stress result convergence. Figure 11 and Figure 12 below depicted the curvatured-based mesh performed on model 1 and the location of stress probed for every simulation run respectively.

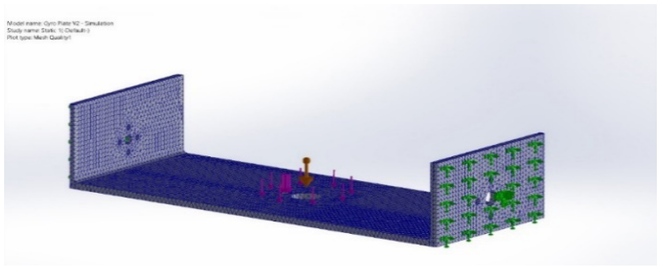

FIGURE 11. Meshing.

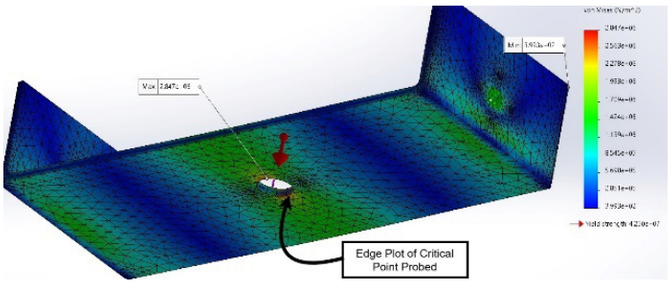

FIGURE 12. Location of Stress Probed.

Next, a mesh convergence study on stress results of each model has been made to ensure the stable solution of the results as mesh become finer. Figure 13 illustrates the process of mesh convergence study done in this research and Table 3 presents the meshing details and the stress results with percentage change as the element size is reduced.

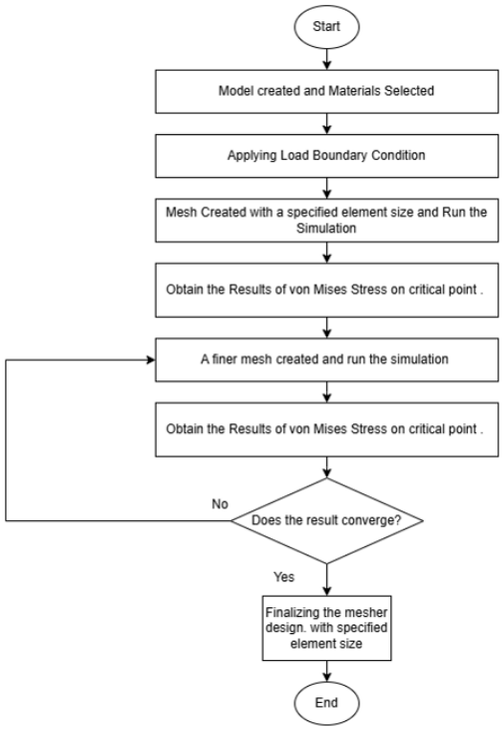

FIGURE 13. Mesh Convergence Study Flowchart

TABLE 3. Meshing Details and Mesh Convergence Results for Model 1-5

Models	Mesh No	Element Size	Number of Nodes	Number of Elements	Nodal Stress Results (N/m^2)	Percentage Change	Convergence (<5%)
	1	15mm	42837	24538	2.77E+06	-	-
1	2	10mm	40167	22707	2.81E+06	2%	Yes
	3	7.5mm	39944	22301	2.85E+06	1%	Yes
	1	15mm	42865	24484	2.27E+06	-	-
2	2	10mm	40453	22807	2.35E+06	4%	Yes
	3	7.5mm	40557	22464	2.39E+06	2%	Yes
	1	15mm	43151	24460	2.44E+06	-	-
3	2	10mm	41575	23274	2.50E+06	3%	Yes
	3	7.5mm	44550	24524	2.49E+06	1%	Yes
	1	15mm	45343	25648	2.30E+06	-	-
4	2	10mm	44605	24778	2.26E+06	2%	Yes
	3	7.5mm	47678	26054	2.30E+06	2%	Yes
	1	15mm	8889	4310	2.07E+06	-	-
5	2	10mm	10915	5295	2.09E+06	1%	Yes
	3	7.5mm	15265	7483	2.18E+06	4%	Yes

As observed in Table 3, the element size of the mesh created in those 3 studies as in Table above has been selected from 15mm to 7.5mm with the reduction of 5mm and 2.5mm. It is chosen to provide consistency in every model as the maximum and minimum element size can be selected is 15mm and 7.5mm respectively. The results employing an element size of the provided range yielded as successive and sufficient mesh refinement with convergence below 5% to capture the behavior of the model accurately while maintaining computational efficiency within acceptable bounds.

As the mesh is refined by reducing the element size, the number of nodes, elements, and nodal stress values increase, reflecting a denser mesh. This increase in nodal stress occurs because finer elements capture stress gradients more accurately, particularly in regions with high stress concentrations. However, as observed in nodal stress result of model 3 and 4, the stress values decrease with finer elements due to stress singularities, where non-physical results arise at sharp edges, corners, or boundary conditions, leading to localized discrepancies in the stress distribution. The element sizes used in the convergence study are deemed acceptable, as convergence was achieved within the range of element sizes tested.

To summary, the successive refinement meshing has been conducted using curvature-based Mesher type with the element shape of octahedral and the element size of 7.5mm is selected for further FEA in observing the von Mises Stress, displacement and strain in the next section.

RESULTS AND DISCUSSIONS

The results of finite element analysis performed on three models of Gyro Plate to obtain minimal stress, resultant deformation and equivalent strain will be discussed in this section. As demonstrated in Figure 14-18, that the middle part of the gyro plate experiences the highest stress and deformation due to the concentrated load from the motor and flywheel except for model 3 where the maximum stress happened to be at the precessional control actuator on the left side of the gyro plate. In terms of strain, Model 1 exhibits the greatest strain output at the corner of the gyro plate, while the other models experience strain near the left side where the actuator is positioned.

FINITE ELEMENT ANALYSIS

The discussion encompasses the FEA conducted by altering the gyro plate's design and substituting the materials from PLA plastics to mild steel or ASTM A36 Steel Plate, one

simulation after another. The thickness of the gyro plate is standardized for every simulation on the different materials which is 4mm. Table 4 below shows the overview of the number of tests run in this research while the analysis and its outcomes are presented in the following sections.

TABLE 4. Overview of Number of Simulation Test on 5 Different Models with 3 Different Materials.

Model	No. of Test	Material Types	Description of Model's Design
1	1	PLA	Basic design for Gyro Plate that satisfies to mount the Gyrostabilizer components; bearing, precession motor and high-speed flywheel motor.
	2	Aluminum	
	3	ASTM A36 Steel	
2	4	PLA	Curved-radial design in the centre at the high-speed motor mounting.
	5	Aluminum	
	6	ASTM A36 Steel	
3	7	PLA	Support added vertically on the bottom side of the gyro plate on both sides.
	8	Aluminum	
	9	ASTM A36 Steel	
4	10	PLA	An additional beam-like supporting along end-to-end of the gyro-plate structure design across left to right
	11	Aluminum	
	12	ASTM A36 Steel	
5	13	PLA	Has a triangular support structure gusset-like shape at the corner.
	14	Aluminum	
	15	ASTM A36 Steel	

MODEL 1

Model 1 is observed to be undeniably without any additional support or extra design for the purpose of holding motor and flywheel in the middle. Upon examination of PLA material for model 1 as in Figure 14, it was determined that the values of von Mises Stress, deformation, and strain, are 2.83 MPa, 1.015mm, and 6.75×10^{-4} respectively. Aluminum Alloy 1060 and ASTM 36 do output a higher stress of 2.93MPa and 3.30MPa in order but lower in deformation of 0.0356mm and 0.0149mm and strain of 2.34×10^{-5} and 9.39×10^{-6} sequentially. This undoubtedly is due to the material mechanical property of higher stiffness (Young's Modulus). To note, compared to other models, the plain design is discerned to be the biggest in FEA results. Regarding the fabrication process using Aluminum or Mild Steel sheet, the design solely entails bending and CNC cutting or laser cutting procedures.

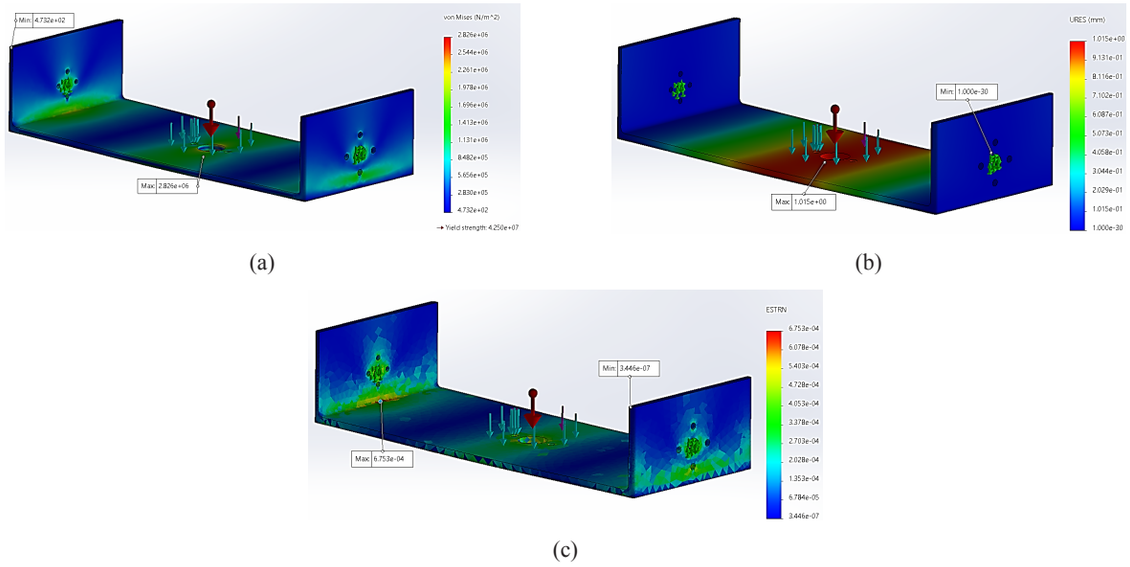

(a) (b)

(c)

FIGURE 14. FEA of Model 1: PLA Material

MODEL 2

Next, the curved-radial design added in the middle of model 2 does reduce the stress and displacement as compared to the plain design. However, strain for aluminum and mild steel material, they still have a small difference bigger value which is unaffecting the design as illustrated in Figure 14 below. In terms of the production, the design only involves the same as model 1 except that the size of the sheet is just a little bigger, leading to a slightly higher production cost.

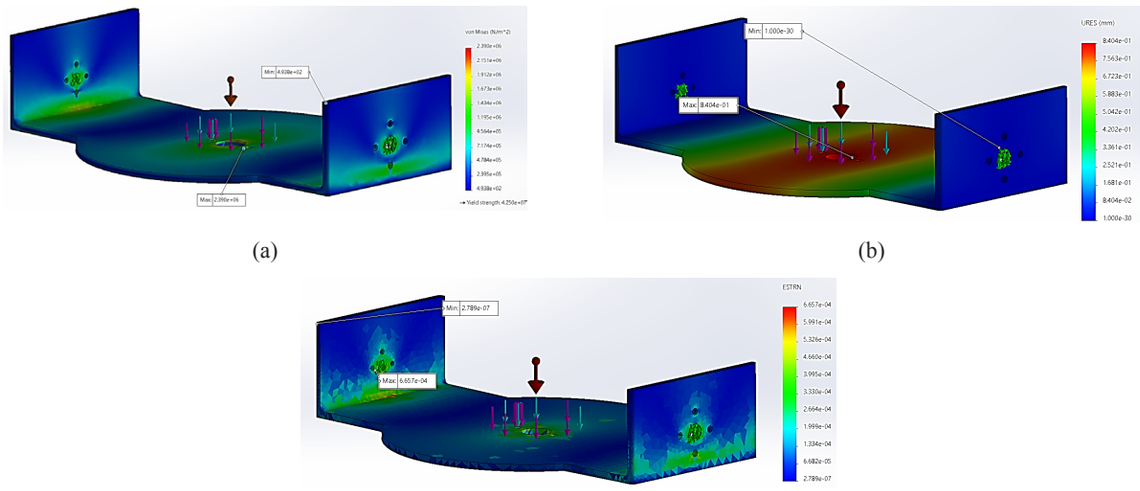

(a) (b)

(c)

FIGURE 15. FEA of Model 2: PLA Material

MODEL 3

On the other hand, model 3 having a support on the bottom side of the gyro plate does not give any significant impact in improving the design. Evidently, the result shows that it gives increment from the model 2 design as indicated in Table 5 and Figure 16 and comparatively close to results as of model 1. Hence, this model explicitly indicates it is not desirable as it just added extra load to the of the gyro plate. Plus, in the production using PLA, it is time consuming in printing while for alloy and steel production, it requires extra sheet and process of unnecessary weldment.

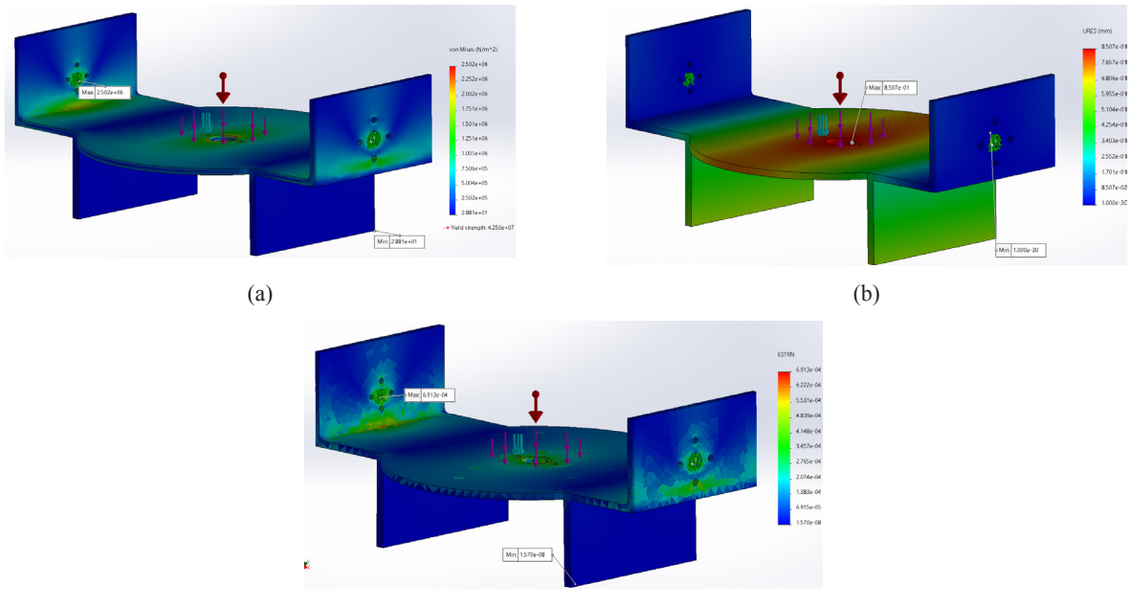

(a) (b)

(c)

FIGURE 16. FEA Model 3: PLA Material

MODEL 4

Model 4 is observably to deliver a serious impact in reduction in all perspectives of Stress, Deformation and Strain when compared to the model 2 design. When compared to the curved model of design 2, the stress has been reduced twice in difference relative to the plain design as such from 2.83MPa to 2.30MPa for PLA design. As for displacement and strain, it does improve in small numbers. Looking into the evaluation of mass properties, model 4 has the biggest volume which directly leads to excessive weight on the assembly. In production perspective, it is identical to the process as in the making of model 3. For this reason, more weight and manufacturing process means a higher production cost. Moreover, it is important to consider the actuator that holds on the left side of the gyro plate, where the higher the components weight, the higher the torque specification of the actuator required. Likewise, it conceivably leads to a much higher in the whole gyrostabilizer production cost.

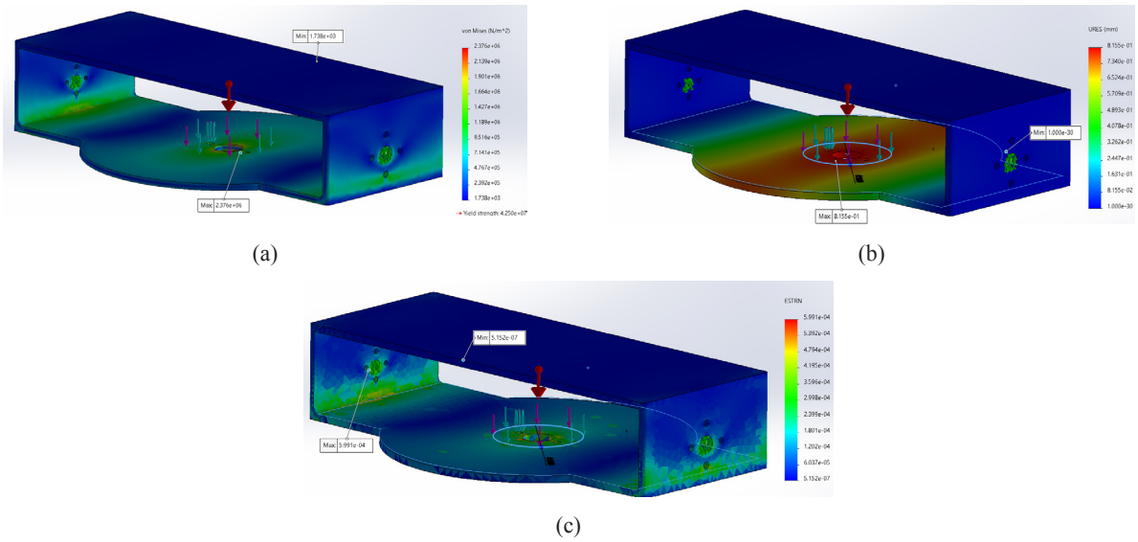

(a) (b)

(c)

FIGURE 17. FEA of Model 4: PLA Material

MODEL 5

Lastly, model 5 which has the triangular support structure gusset-like shape at the corner of the gyro plate results in more improvement from all the previous design. The stress has been able to reduce to almost 2MPa for PLA and 1060 Alloy. As for mild steel, the von Mises Stress does not reduce and still maintains about 3.25MPa, closer to plain design from model 1. This might be due to the design of the gusset-like support may not be sufficient to effectively redistribute the applied loads and support the corner of the gyro plate. Despite this, the displacement or deformation did improve well to the lowest value in all designs in contrast. For strain, all model 5 of these 3 material types maintain about the same as model 1 which is acceptable. Delving into the production and process, PLA has no problem since 3D-printing is capable of printing it vertically upwards easily. As for alloy and steel sheet, it requires welding process added on top of the bending corner section of the design. Logically, it is possible but a vexing process since more welding might lead to unwanted bending on the design itself.

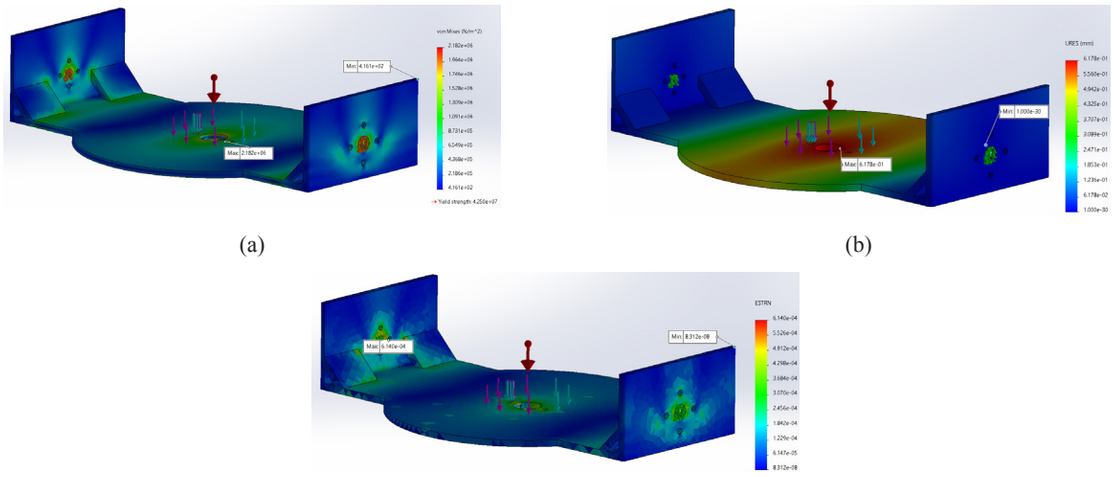

(a) (b)

(c)

FIGURE 18. FEA Model 5: PLA Material

TABLE 5. Results of FEA Analysis on 5 model of 3 different types of materials

Model	Case	Type	Stress von Misses (N/m^2)		Displacement(mm)		Strain	
			Max	Min	Max	Min	Max	Min
1	1	PLA Pro	2.83E+06	2.601E+02	1.02E+00	1.00E-30	6.75E-04	3.45E-07
	2	1060 Alloy	2.93E+06	4.51E+02	3.56E-02	1.00E-30	2.34E-05	9.42E-09
	3	Mild Steel/ ASTM 36	3.30E+06	4.24E+02	1.49E-02	1.00E-30	9.39E-06	2.58E-09
2	1	PLA Pro	2.39E+06	4.94E+02	8.40E-01	1.00E-30	6.66E-04	2.79E-07
	2	1060 Alloy	2.50E+06	5.11E+02	3.02E-02	1.00E-30	2.38E-05	8.02E-09
	3	Mild Steel/ ASM 36	3.08E+06	4.54E+02	1.34E-02	1.00E-30	1.04E-05	2.66E-09
3	1	PLA Pro	2.49E+06	2.49E+01	8.45E-01	1.00E-30	6.48E-04	2.75E-08
	2	1060 Alloy	2.74E+06	5.28E+01	3.06E-02	1.00E-30	2.35E-05	7.93E-10
	3	Mild Steel/ ASM 36	3.72E+06	1.09E+02	1.40E-02	1.00E-30	1.06E-05	3.15E-10
4	1	PLA Pro	2.30E+06	1.35E+03	8.15E-01	1.00E-30	5.99E-04	8.19E-07
	2	1060 Alloy	2.48E+06	2.87E+03	2.92E-02	1.00E-30	2.13E-05	4.19E-08
	3	Mild Steel/ ASM 36	2.38E+06	1.74E+03	8.16E-01	1.00E-30	5.99E-04	5.15E-07
5	1	PLA Pro	2.18E+06	3.52E+02	6.18E-01	1.00E-30	6.41E-04	7.27E-08
	2	1060 Alloy	2.33E+06	3.80E+02	2.20E-02	1.00E-30	2.30E-05	2.41E-09
	3	Mild Steel/ ASM 36	3.25E+06	5.04E+02	9.64E-03	1.00E-30	1.01E-05	1.11E-09

Viewing from a materials perspective, PLA outputs minimal stress but comparatively high in displacement and strain compared to aluminum alloy and mild steel. Figure 19-21 depict a well picture of comparison by models and materials. It is undeniable that the facts of PLA's characteristics having significantly lower Young's modulus with flexible molecular structure but relatively compared to aluminum alloy and mild steel, making it less resistant to deformation under stress. Hence, it tends to deform

plastically and absorb energy through strain, resulting in higher overall displacement as compared to metals.

In contrast, aluminum alloy and mild steel, with their higher Young's modulus and superior structural stiffness, exhibit lower displacement and strain under similar stress conditions. These materials demonstrate greater resistance to deformation, which is crucial for maintaining the structural integrity of the gyro plate under operational loads.

As observed from FEA results of model 5 results, a displacement of 0.618mm is relatively small, even for PLA suggesting that this material could potentially be used for designing a gyro plate on a small 1-meter vessel, particularly for lightweight applications. 0.618mm is quite a small value in displacement to be considered even if it is a PLA. However, its mechanical limitations, such as higher displacement and strain under stress, must be carefully considered to ensure performance and structural reliability in such environments. The use of aluminum alloy or mild steel offers a more reliable solution for such applications due to their ability to withstand higher stresses and maintain stability under load.

Overall, the analysis highlights the importance of material selection for gyrostabilizer design. The convergence observed in stress, displacement, and strain values across different models further validates the accuracy of the FEA study, providing confidence in the results. This ensures the design feasibility and performance expectations for the gyro plate in contributing to the stability of the 1-meter boat.

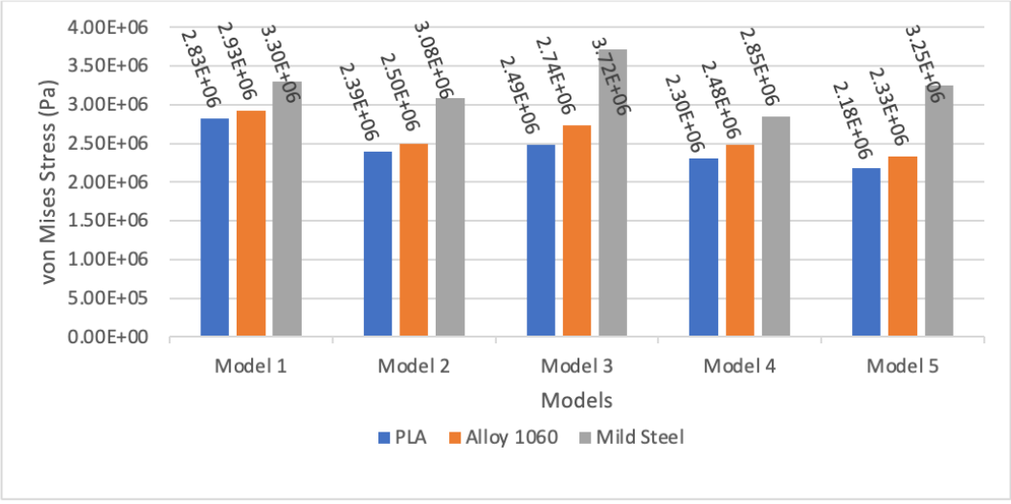

FIGURE 19. von Mises Stress Comparison on Gyro Plate Models based on Different Materials

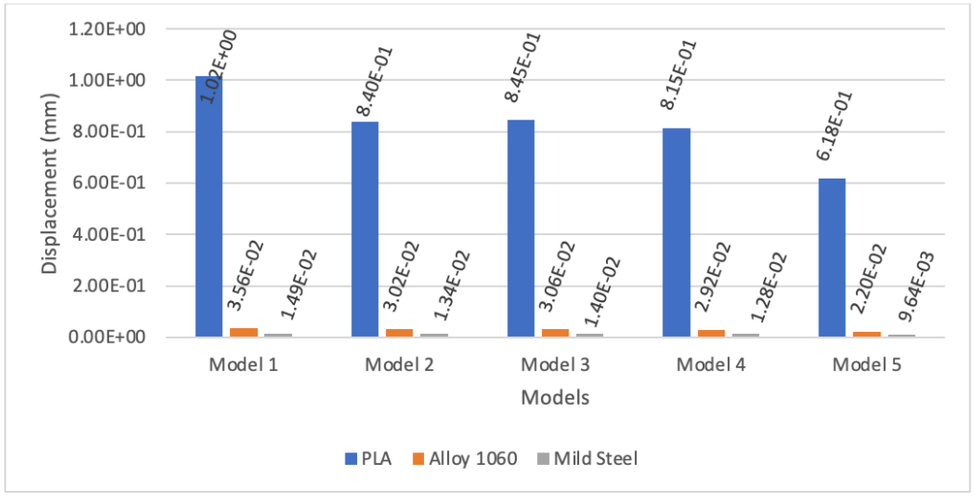

FIGURE 20. Displacement Comparison on Gyro Plate Models based on Different Materials

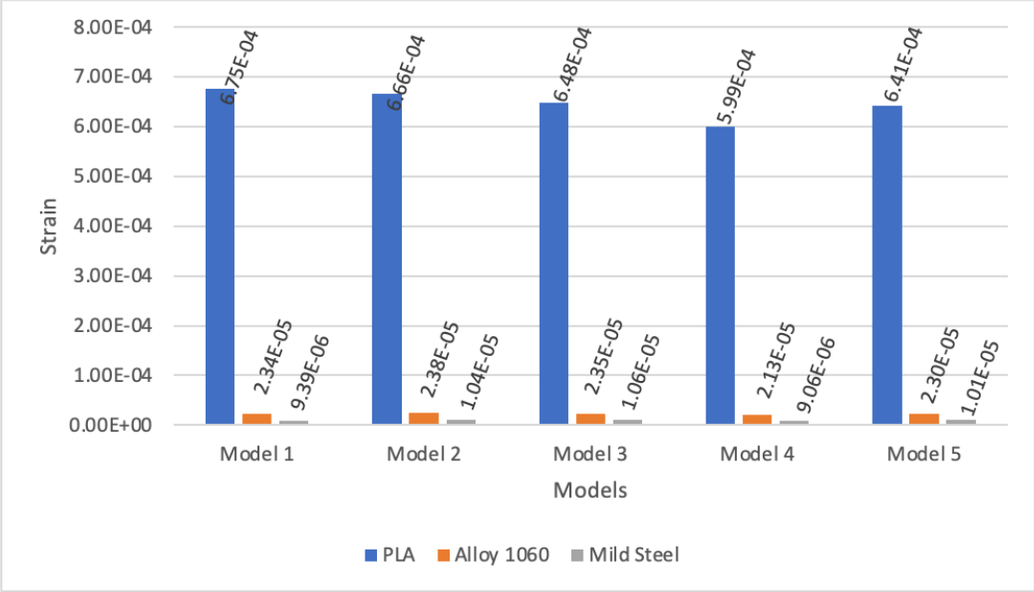

FIGURE 21. Strain Comparison on Gyro Plate Models based on Different Materials

CONCLUSIONS

Five different gyro plate models were designed and analyzed using the Finite Element Method in SOLIDWORKS with three materials: PLA Pro, 1060 Aluminum Alloy, and Mild Steel/ASTM 36. The results, which focused on stress, deformation, and strain, revealed progressive improvements from Models 1 to 5, except for Model 3. Model 3 showed no significant benefits and was inefficient in terms of production time.

Models 1 and 2 stood out for their simplicity in manufacturing. They could be fabricated through bending (for sheet metals) or additive manufacturing (for PLA), making them cost-effective for production. Model 2 achieved a noticeable reduction in stress and deformation due to the slight addition of a curve-shaped feature, demonstrating a balance of performance and manufacturability. Model 5 emerged as the most effective design, achieving the lowest stress, deformation, and strain values across all materials. For instance, with PLA, the displacement was reduced to 0.618 mm and stress to 2.18 MPa, outperforming all other designs. Although manufacturing Model 5 in aluminum or mild steel may pose challenges due to the need for welding, its compatibility with 3D printing makes it a feasible choice for PLA production, as it involves only bending processes and avoids additional fabrication methods.

Looking ahead, the application of 3D printing to manufacture a larger gyro plate for use in bigger vessels or boats offers significant potential. This exploration could extend the design's applicability to larger-scale stabilization systems. Future work should include experimental validation of the proposed design to confirm its performance in real-world conditions.

ACKNOWLEDGEMENT

The author, Harith Aslam wishes to express his gratitude to all parties who were directly or indirectly involved in this effort, particularly the IIUM Centre for Unmanned Technologies (CUTe) lab for providing equipment. This initiative was also made possible by the community of IIUM and facilities provided by Robot Design Lab. Next, the author also acknowledges the support of the TFW2021 scheme of Kulliyyah of Engineering, International Islamic University Malaysia.

DECLARATION OF COMPETING INTEREST

None.

REFERENCES

Arutyunov, S. S. 1960. Errors of a single-degree-of-freedom integrating gyro due to angular oscillations of its base. *ARS Journal 30*(7): 661–662. https://doi.org/10.2514/8.5179

Beznos, A. V., Formal'sky, A. M., Gurfinkel, E. V., Jicharev, D. N., Lensky, A. V., Avitsky, K., & Tchesalin, L. S. 1998. Control of autonomous motion of two-wheel bicycle with gyroscopic stabilisation. *Proceedings - IEEE International Conference on Robotics and Automation 3*(May): 2670–2675. https://doi.org/10.1109/ROBOT.1998.680749

Deleanu, D., Dumitrache, C. L., & Turof, M. 2022. Control of ship fin stabilizers by a PID controller: A numerical analysis. *International Journal of Modern Manufacturing Technologies* 14(2): 40–47. https://doi.org/10.54684/ijmmt.2022.14.2.40

Diniz, C. A., Méndez, Y., de Almeida, F. A., da Cunha, S. S., & Gomes, G. F. 2021. Optimum design of composite structures with ply drop-offs using response surface methodology. *Engineering Computations (Swansea, Wales):* 38(7): 3036–3060. https://doi.org/10.1108/EC-07-2020-0354

Gogoi, P., Nath, M., Doley, B. T., Boruah, A., & Barman, H. J. 2017. Design and fabrication of self balancing two wheeler vehicle using gyroscope. *International Journal of Engineering and Technology* 9(3): 2051–2058. https://doi.org/10.21817/ijet/2017/v9i3/1709030206

Hung, L. K., Lee, C. H., & Su, K. C. 2021. Biomechanical analysis of clavicle hook plates with a range of posterior hook offsets implanted at different acromion positions in the acromioclavicular joint: A finite element analysis study. *Applied Sciences (Switzerland):* 11(23). https://doi.org/10.3390/app112311105

Jagota, V., Preet, A., Sethi, S., & Kumar, K. 2013. Finite Element Method: An overview. *Walailak J Sci & Tech* 10(1). http://wjst.wu.ac.th

Jianhui, L. U., & Shaonan, C. H. E. N. 2011. Active gyro-stabilizer for nonlinear roll suppression of marine vehicles. *Journal of Mechanical Engineering* 47(19): 86–90. https://doi.org/10.3901/JME.2011.19.086

Karagiannis, I. 2015. *Design of Gyro Based Roll-Stabilization Controller for a Concept Amphibious Commuter Vehicle* (Issue June).

Lenartowicz, A., Przychodzki, M., Guminiak, M. & Garbowski, T. (2021). Optimal placement of viscoelastic vibration dampers for kirchhoff plates based on pso method. *Materials* 14(21). https://doi.org/10.3390/ma14216616

Li, B., Zhang, X., Wang, J., & Chen, N. 2022. Anti-roll characteristics of marine gyrostabilizer based on adaptive control and hydrodynamic simulation. *Journal of Marine Science and Engineering* 10(1). https://doi.org/10.3390/jmse10010083

Liu, W. K., Li, S., & Park, H. S. 2022. Eighty years of the finite element method: Birth, evolution, and future. *Archives of Computational Methods in Engineering* 29(6): 4431–4453. https://doi.org/10.1007/s11831-022-09740-9

Manmathakrishnan, P., & Pannerselvam, R. 2019. Design and Performance evaluation of Single axis gyrostabilizer for motion stabilization of a scaled Barge model. *OCEANS 2019 MTS/IEEE Seattle, OCEANS 2019*. https://doi.org/10.23919/OCEANS40490.2019.8962634

Md Tahir, M., Juki, I., Yong, L. H., Mohammad, S., & Ngian, S. P. 2011. Finite element analysis of flush end-plate connections connected to column web. *International Journal of Steel Structures* 11(3): 247–258. https://doi.org/10.1007/s13296-011-3001-3

Müller, R. D., Sdrolias, M., Gaina, C., & Roest, W. R. 2008. Age, spreading rates, and spreading asymmetry of the world's ocean crust. *Geochemistry, Geophysics, Geosystems* 9(4). https://doi.org/10.1029/2007GC001743

Naziri, H. A. A., & Ibrahim, A. I. 2022. Multi-Stabilizer Devices for Marine Vessel, Design and Control-A Review. *2022 IEEE 9th International Conference on Underwater System Technology: Theory and Applications, USYS 2022*. https://doi.org/10.1109/USYS56283.2022.10072471

Nguyen, N. H., Do, V. P., & Vu, H. T. 2022. Estimating disturbance torque effects on the stability and control performance of two-axis gimbal systems. *Journal of the Russian Universities. Radioelectronics* 25(4): 63–71. https://doi.org/10.32603/1993-8985-2022-25-4-63-71

Nurrohmad, A., Antares, Q., Nuranto, A. R., & Nugroho, A. 2024. Optimization of double hole composite plate on the floater compartment of amphibious aircraft using Taguchi Method. *WARTA ARDHIA* 49(2): 87. https://doi.org/10.25104/wa.v49i2.520.87-95

Park, J. H., & Cho, B. K. 2018. Development of a self-balancing robot with a control moment gyroscope. *International Journal of Advanced Robotic Systems* 15(2): 1–11. https://doi.org/10.1177/1729881418770865

Pavlidis, A., & Rowe, D. n.d. *The Sporting Bubble as Gilded Cage Gendered Professional Sport in Pandemic Times and Beyond Introduction: Bubbles and Sport*. https://doi.org/10.5204/mcj.2736

Poh, A. K. B., Tang, C. H. H., Kang, H. S., Lee, K. Q., Siow, C. L., Malik, A. M. A., & Mailah, M. 2018. Gyroscopic stabilisation of rolling motion in simplified marine hull model. *2017 IEEE 7th International Conference on Underwater System Technology: Theory and Applications, USYS 2017*, *2018-Janua*(December): 1–6. https://doi.org/10.1109/USYS.2017.8309458

Talha, M., Asghar, F., & Kim, S. H. 2017. Design of fuzzy tuned PID Controller for Anti Rolling Gyro

(ARG) stabilizer in ships. *International Journal of Fuzzy Logic and Intelligent Systems* 17(3): 210–220. https://doi.org/10.5391/IJFIS.2017.17.3.210

Virág, Z., & Szirbik, S. 2021. Modal analysis of optimized trapezoidal stiffened plates under lateral pressure and uniaxial compression. *Applied Mechanics* 2(4): 681–693. https://doi.org/10.3390/applmech2040039

Wang, S., Sun, Y., Chen, H., & Han, G. 2017. Kinematics and force analysis of a novel offshore crane combined compensation system. *Proceedings of the Institution of Mechanical Engineers Part M: Journal of Engineering for the Maritime Environment* 231(2): 633–648. https://doi.org/10.1177/1475090216679256

Zhang, S., Lu, D., Huang, M., Li, R., Li, Z., & Xu, W. 2024. Research on the lightweight design and multilevel optimization method of B-pillar of hybrid material based on side-impact safety and multicriteria decision-making. *Polymer Composites* 45(5): 4051–4077. https://doi.org/10.1002/pc.28042

Zhang, T. A. O. 2014. *Analysis of Active Gyro Based Roll-Stabilization of Slender Boat Hulls*. School of Engineering Sciences (SCI)